AD-A167 903 TECHNIQUES FOR EARLY CHARACTERIZATION OF BURN INJURIES (U) WASHINGTON UNIV SEATTLE DEPT OF ELECTRICAL ENGINEERING M A AFROMOWITZ 30 NOV 82 DAMD17-80-C-0147 1/1

UNCLASSIFIED F/G 6/12 NL

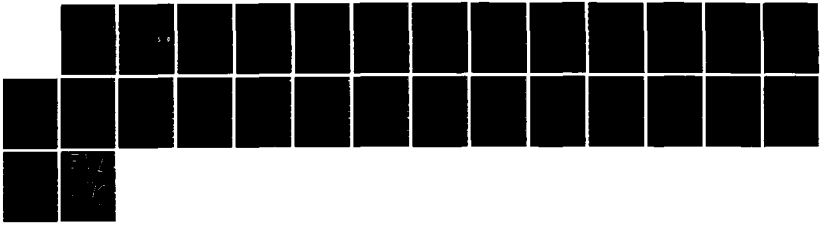

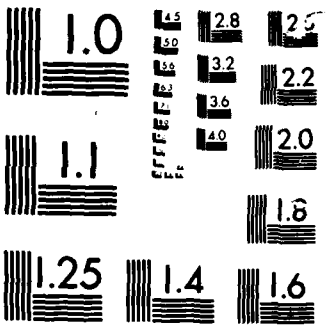

MICROCOPY CHART

PHOTOGRAPH THIS SHEET

AD-A167 903

DTIC ACCESSION NUMBER

LEVEL

REPORT BI-2

TECHNIQUES FOR EARLY CHARACTERIZATION OF BURN INJURIES

ANNUAL PROGRESS REPORT

DOCUMENT IDENTIFICATION

(1)

INVENTORY

DISTRIBUTION STATEMENT A
Approved for public release;
Distribution Unlimited

DISTRIBUTION STATEMENT

ACCESSION FOR		
NTIS	GRA&I	☑
DTIC	TAB	☐
UNANNOUNCED		☐
JUSTIFICATION		
BY		
DISTRIBUTION /		
AVAILABILITY CODES		
DIST	AVAIL AND/OR SPECIAL	
A-1		

DISTRIBUTION STAMP

DTIC
ELECTE
JUN 03 1986
S D
D

DATE ACCESSIONED

DATE RETURNED

86 6 3 002

DATE RECEIVED IN DTIC

REGISTERED OR CERTIFIED NO.

PHOTOGRAPH THIS SHEET AND RETURN TO DTIC-DDAC

DTIC FORM 70A DEC 83

DOCUMENT PROCESSING SHEET

PREVIOUS EDITION MAY BE USED UNTIL STOCK IS EXHAUSTED.

DRAFT
Do Not Cite Or Quote

AD _____

REPORT NUMBER BI-2

TECHNIQUES FOR EARLY CHARACTERIZATION OF BURN INJURIES

ANNUAL PROGRESS REPORT

Martin A. Afromowitz
Department of Electrical Engineering
University of Washington

November 30, 1982

Supported by

U. S. ARMY MEDICAL RESEARCH AND DEVELOPMENT COMMAND
Fort Detrick, Frederick, Maryland 21701

Contract No. DAMD-17-80-C-0147

University of Washington
Seattle, Washington 98195

UNCLASSIFIED

SECURITY CLASSIFICATION OF THIS PAGE (When Data Entered)

REPORT DOCUMENTATION PAGE		READ INSTRUCTIONS BEFORE COMPLETING FORM
1. REPORT NUMBER	2. GOVT ACCESSION NO.	3. RECIPIENT'S CATALOG NUMBER
4. TITLE (and Subtitle) Techniques for Early Characterization of Burn Injuries		5. TYPE OF REPORT & PERIOD COVERED May 16, 1981 - August 31, 1982 Annual Progress Report 6. PERFORMING ORG. REPORT NUMBER
7. AUTHOR(s) Martin A. Afromowitz		8. CONTRACT OR GRANT NUMBER(s) DAMD-17-80-C-0147
9. PERFORMING ORGANIZATION NAME AND ADDRESS Department of Electrical Engineering University of Washington Seattle, WA 98195		10. PROGRAM ELEMENT, PROJECT, TASK AREA & WORK UNIT NUMBERS
11. CONTROLLING OFFICE NAME AND ADDRESS U.S. Army Medical Research and Development Command SGRD-RMS Fort Detrick, Frederick, MD 21701		12. REPORT DATE November 30, 1982 13. NUMBER OF PAGES
14. MONITORING AGENCY NAME & ADDRESS(if different from Controlling Office) Letterman Army Institute of Research SGRD-ULZ-RCM Presidio of San Francisco San Francisco, CA 94129		15. SECURITY CLASS. (of this report) UNCLASSIFIED 15a. DECLASSIFICATION/DOWNGRADING SCHEDULE

16. DISTRIBUTION STATEMENT (of this Report)

Approved for public release; distribution unlimited

17. DISTRIBUTION STATEMENT (of the abstract entered in Block 20, if different from Report)

18. SUPPLEMENTARY NOTES

19. KEY WORDS (Continue on reverse side if necessary and identify by block number)

Burn injury
Burn depth
Doppler ultrasound
Optical methods
Wound healing
Skin blood flow

20. ABSTRACT (Continue on reverse side if necessary and identify by block number)

There are at present no objective methods available to medical personnel to quantitatively characterize the depth of burns or to accurately estimate the time required for healing. This information is crucial in the early stages of burn care since it determines whether or not surgical procedures are required. Our research is directed at the development of two non-invasive tools for characterizing burns during the first hours or days following injury. The first device measures the optical reflection properties of the burn and correlates this measure with healing time. The second instrument measures skin

DD FORM 1 JAN 73 1473 EDITION OF 1 NOV 65 IS OBSOLETE

UNCLASSIFIED

SECURITY CLASSIFICATION OF THIS PAGE (When Data Entered)

blood flow patterns as a function of depth below the surface of the burn using Doppler ultrasound techniques.

Statement of the Problem

The problem addressed by the research reported on herein is concerned with the development and testing of two different non-invasive instruments for the early characterization of burns. An electro-optic burn depth indicator developed by the author quantitatively measures the red, green, and infrared reflectivity of a burn. We proposed to test this instrument on burns during the first few days post-burn, and determine whether this instrument has value in diagnosing burn depth when used in that time frame.

The second aspect of our program is concerned with developing a new instrument, the 20 MHz pulsed Doppler ultrasound skin blood flow indicator. This instrument was designed to detect and measure the characteristics of skin blood flow as a function of depth below the surface of a burn wound. It is expected that this information can be used to evaluate zones of stasis and predict eventual burn wound healing.

The research is directed toward the development of inexpensive portable instruments which can be used as aides in determining burn depth and estimating "time to healing" and are intended to be used as diagnostic tools to help characterize burn wounds, select the appropriate treatment modality, and to monitor healing processes.

Background

We have shown in previous work [1] that the time required for a burn wound to heal (e.g., less than or greater than three weeks healing time) is strongly correlated with the optical reflection properties of the wound when measured quantitatively between three and seven days post-burn. In our instrument, red, green, and near infrared light is focused on a small selected area of the burn wound, and the reflected intensities are measured automatically. Ratios of the reflected intensities (red to infrared, and green to infrared) are derived electronically and displayed. When these data are plotted on a graph as shown in Figure 1, we find that points representing measurements made on burns that eventually heal in less than three weeks (x's) generally fall above the dividing line shown on the figure. Points representing measurements on burns that require grafting, or on burns that take longer than three weeks to heal (o's) generally fall below the dividing line.

Several parameters may affect the accuracy of this correlation. These parameters include the age and sex of the patient, the location, etiology and extent of burn, presence of blood (denatured or not), number of days post-burn, etc. Our goal is to determine how these parameters affect the optical properties of the burn, and whether accurate predictions of burn depth or "time to healing" can be made within the first few days post-burn, using the electro-optic burn depth indicator.

The second approach to burn characterization involves the detection and measurement of the minute flow of blood in the intact capillary loops, and arteriolar and venous plexi which remain after the burn injury. This flow can be detected by means of the Doppler shift of 20 MHz ultrasound waves which we direct at small areas of the skin by means of a tiny transducer, and which reflect from the blood cells moving through the vascular system of the tissue. The injured tissue can be probed at different levels below the surface with a

depth resolution of approximately 0.4 mm. The characteristics of the blood flow at each level can be measured. This information is expected to correlate very well with the eventual healing pattern of the burn wound.

Approach

Our approach involves a five year plan of research, instrument development, clinical tests, and analysis. The first year of this project was devoted to:

1) Clinical tests on the electro-optic burn depth instrument, conducted at the Burn Center of Harborview Medical Center under the direction of Dr. David Heimbach, Director of the Burn Center, and Dr. Loren Engrav, Department of Surgery. The purpose was to start to accumulate a large data base so that we could correlate the optical properties of burns with the various parameters mentioned above;

2) Design and construction of the 20 MHz Doppler ultrasound instrument;

3) Initial characterization of the ultrasound instrument and modifications based upon our experience with it.

During the second year of this project, our efforts included:

1) Continuation of the clinical tests on the electro-optic burn depth instrument, conducted at the Burn Center of Harborview Medical Center. A total of more than 75 patients were included in our study.

2) Analysis of the data obtained with the electro-optic burn depth instrument for several categories of burns.

3) Tests of the ultrasound skin blood flow instrument on normal skin at one particular body location (finger pad).

4) Analysis of the information present in the Doppler spectrum of the ultrasound instrument, and identification of specific features of the spectrum with microvascular structures in the skin, as well as blood flow characteristics.

The results of our work during the second year of this program will be discussed below.

Succeeding years of this project will be devoted to continued clinical testing of the electro-optic instrument, development of clinically-compatible transducers for the ultrasound instrument, a clinical test program using the ultrasound measurements as predictors of burn depth or "time to healing", and design and construction of self-contained, compact instruments with simple output indicators for ultimate use by inexperienced personnel as an aide in diagnosing burn injuries and selecting appropriate treatment.

Part I: The Electro-Optic Burn Depth Instrument

Well over 1500 measurements of the optical properties of specific burn sites were made on approximately 75 patients. The measurements and site selections

were made by our research nurse, Ms. Perry. Site selection was made with the objective of accumulating a data base with the widest possible variation in burn characteristics. After site selection, the patient was photographed with instant color film, and the sites were located for future reference by number on the photographs. Measurements were made on the same sites on each patient on each post-burn day the patient was available during the first week post-burn.

Each burn site was categorized according to the following parameters:

1) Age of patient
2) Sex of patient
3) Etiology of the burn (chemical, flame, contact, electrical, scald)
4) Presence of any complicating medical condition
5) Total percentage second plus third degree burn area
6) Body part, one of six groupings, including
    a) head and neck
    b) arms, including axilla
    c) anterior abdomen, chest, and pubis
    d) back
    e) legs, including gluteii
    f) hands and feet
7) Day post-burn of the measurement

In addition, each site was clinically evaluated by the burn surgeon at the earliest possible opportunity, and a record was made of the clinical evaluation, which constituted a statement as to whether the particular burn site was expected to heal in three weeks or not, or that the clinical signs were not clear enough to make a guess.

Each burn site was followed clinically by the burn research nurse. If the site healed (an event marked by complete epithelial cell coverage), the number of days until healing was recorded. If the site was excised, the burn nurse accompanied the patient to surgery, and when the surgeon excised the site he was asked to judge whether or not the site would have had any chance to heal within the three week post-burn period. There were five possible outcomes at this point:

1) The site was clearly third degree, and no healing could have been expected.
2) The site probably would not have healed in three weeks.
3) Still do not know if it would have healed in three weeks.
4) Probably would have healed were it not excised.
5) A mosaic burn, excised and grafted for surgical ease, faster healing, and prevention of contractures.

All the burn site parameters described above, including the optical measurements made on each site on each post-burn day, were stored in our data file. A computer program permits us to select all the burn sites that conform to any set of selected parameter values, and plot the optical measurement data of these sites. The data is plotted as in Figure 1, with the red/infrared reflectivity ratio on the y-axis, and the green/infrared reflectivity ratio on the x-axis. It is observed that there is a strong correlation of the position of a data point with the ultimate healing behavior of the burn site. We shall describe some of these results shortly.

We should note that in some cases it is difficult to know whether a particular

burn site should be characterized as one which would or would not heal in a period of three weeks if not excised. Clearly those burns that were excised and at the time of surgery could not be absolutely designated as third degree burns fall into this questionable group. In the analyses presented below, we shall refer only to burns with "confirmed" outcomes. This includes only those burns which were not excised (hence, their "time to healing" is known accurately) and those burns excised and judged to be "clearly third degree" during the excision procedure.

Results and Discussion

During the seventh quarter of our research program, an analysis of our electro-optic data file was undertaken. Most of the burn categories did not have enough data to permit strong conclusions to be made. However, in the case of burns of the hands and feet including all patients for which confirmed outcomes are available (all etiologies, ages, etc.), several striking conclusions can be drawn. The analysis is as follows.

Figure 1 shows the optical data on burn sites which meet the following criteria:

> Burns of the hands or feet with confirmed outcomes;
> Data taken on post-burn day 2;
> The burn surgeon's clinical evaluation (initially) was: this burn will heal in three weeks without surgical intervention.

Those data points measured on burn sites that eventually healed within 21 days are plotted with a cross (x); those data points measured on sites that did not or would not have healed in 21 days are plotted with a circle (o). A dividing line is shown drawn through the data points. Out of the 34 burn sites that meet the stated criteria, 23 sites eventually healed in 21 days, and 11 sites did not. Of the 23 that healed, 22 of the data points fall above the dividing line. Of the 11 sites that did not heal, 7 of the data points fall below the dividing line.

Figure 2 is similar to Figure 1, but in this case, burn sites were selected based upon the following criteria:

> Burns of the hands or feet with confirmed outcomes;
> Data taken on post-burn day 2;
> Initial clinical evaluation: cannot tell whether the burn will or will not heal in three weeks without surgical intervention.

Of the 17 sites in this category, 13 healed in 21 days, and 4 did not or would not have healed in 21 days. Of the 13 sites that healed, 10 had data points that fell above the same dividing line as used in Figure 1. Of the 4 sites that did not heal, 3 had data points that fell below the dividing line.

Only one burn site met the following criteria:

> Burns of the hands or feet with confirmed outcomes;
> Data taken on post-burn day 2;
> Initial clinical evaluation: will not heal in three weeks.

The data point for this site fell above the dividing line. No figure is shown

for this one point.

The data presented above can be summarized as follows:

1) There were 36 cases in which the burn site healed in 21 days. Of these, the initial clinical evaluation by the burn surgeon was correct in 23 cases, never incorrect, and in 13 cases no guess could be made.

2) There were 16 cases in which the burn sites did not heal in 21 days. Of these, the initial clinical evaluation was correct in 1 case, incorrect in 11 cases, and no guess was made in 4 cases.

In order to judge the potential capabilities of the electro-optic burn depth instrument in predicting burn healing times, we evaluate our measured data in the following way: if the data point falls above the dividing line, we shall predict that the site will heal in 21 days; if the data point falls below the line, we shall predict that the site will not heal in 21 days. Using this criteria:

1) Of the 36 cases of confirmed burn healing in 21 days, the electro-optic burn depth indicator was correct in 32 cases and incorrect in 4 cases.

2) Of the 16 cases of confirmed non-healing, the electro-optic burn depth indicator was correct in 10 cases and incorrect in 6 cases.

Table 1 summarizes these results.

	Burn surgeon's initial evaluation			Electro-optic instrument	
	correct	incorrect	no guess	correct	incorrect
Healers (36 cases)	64%	0%	36%	89%	11%
Non-healers (16 cases)	6%	69%	25%	63%	37%

TABLE 1. Post-burn day 2, data of the hands and feet

A similar analysis was performed for burns of the hands and feet in which data was taken on post-burn day 3. The summary of results is shown in Table 2:

	Burn surgeon's initial evaluation			Electro-optic instrument	
	correct	incorrect	no guess	correct	incorrect
Healers (28 cases)	50%	0%	50%	96%	4%
Non-healers (17 cases)	6%	70%	24%	82%	18%

TABLE 2. Post-burn day 3, data of the hands and feet

Thus, by comparing the accuracy of prediction for the electro-optic burn depth instrument with that of the surgeon's initial guess, the instrument is clearly superior for this particular burn category. The instrument's predictions were better on day 3 than on day 2 post-burn. We hasten to note that the

clinical evaluations were made on day 1 or 2 post-burn. It is very possible that clinical evaluations would be more correct were they made on day 3 or 4 post-burn, after the burn wound stabilized. However, the results presented suggest very strongly that the electro-optic burn depth instrument can be useful in the early characterization of burn wounds. Obviously, a great deal more data must be accumulated and analyzed before we can define the overall accuracy of this technique for burns in all the different categories.

Part II: The Doppler Ultrasound Skin Blood Flow Instrument

During the period covered by this Annual Progress Report, we made significant progress in evaluating the use of pulsed Doppler ultrasound for the measurement of skin blood flow. This technique offers potential advantages over the electro-optic technique described above in that

1) the ultrasound technique may be used to assess wound healing in cases other than burns,

2) the technique is usable in burn wounds whose surface is not prepared in a standard manner (e.g., freshly cleaned, no anti-bacterial creams applied, etc.), and

3) the technique measures a physiologically-important parameter directly, whereas the electro-optic instrument measures an integrated effect of the light scattering characteristic of the tissue.

The following sections describe our research efforts devoted to the development of the ultrasound technique.

Introduction

Skin blood flow is an important parameter in a number of physiological processes, including healing of wounds due to burn injuries or other injuries, skin diseases, thermal regulation, skin nutrition, and so on. A number of methods have been developed in an attempt to quantify this parameter: radioactive isotope clearance [2], plethysmography [3], and laser Doppler [4-7] to name a few. Of these methods, the laser Doppler instrument is the simplest to use and has the benefit of being noninvasive. In this report a new method of skin blood flow measurement using pulsed Doppler ultrasound is discussed. Initial data presented in this report indicate that parameters relating to skin blood flow appear in the output of a Doppler ultrasound flow detector.

Our research has been aimed at identifying unique Doppler flow patterns at specific depths in the skin, and correlating these patterns with the vessel structure at that depth. Since the ultrasonic wave speed in tissue is approximately 1500 m/sec, the ultrasound Doppler instrument can open its receiver gate at a selectable delay with respect to the transmitted burst, thus allowing scattered signals from varying depths to be distinguished. This feature contrasts with the limitation of the laser Doppler instrument which due to the speed of light must operate in a continuous wave mode, and thus reflections from different depths cannot be distinguished. A Doppler ultrasound instrument possessing the capability to identify structures at different depths in the skin could conceivably be of use in evaluating the depth of skin damage due to a burn injury.

Methods

The instrument used in all investigations is a 20 MHz pulsed Doppler ultrasound flow detector [8], with a depth resolution of about 0.4 mm. The major feature of this instrument is the ability to eliminate small amplitude, relative motion artifacts between the transducer and the skin. This is accomplished by initiating both the clock phase and receiver gate delay circuitry by the first received reflection (skin surface) after the transmit burst. Thus, when the skin surface moves with respect to the transducer because of plethysmographic effects or muscle tremors beneath the skin, the reference point for the clock phase and the receiver gate also moves, and thus the receiver gate always stays at the same depth in the skin. Therefore, only motion relative to the skin surface should give Doppler shifted frequency components in the ultrasound output. Blood cells, vessel walls and interfaces within the skin will all give Doppler components in the output since their motion may not follow the motion of the skin surface (stratum corneum).

All measurements were performed in vivo on a 24 year old male volunteer using the right hand middle finger pad as the area of observation. The finger was chosen as the observation point for a number of reasons. First, it has a high degree of perfusion in relation to other areas of the body. Second, the finger can be held easily (as shown in Figure 3) by a simple test tube clamp, and the transducer can be aimed directly at the finger pad. Finally, blood flow in the finger can be varied considerably by immersing the hand in warm water, or by inflating a pressure cuff above the elbow (arterial occlusion). A typical range of skin thickness in the finger, from stratum corneum to the dermis - subcutis interface, is 0.7 mm to 1.4 mm.

In all the investigations presented here, the audio output of the ultrasound device was tape recorded with a recording bandwidth of 0 to 312 Hz on an HP396A FM instrumentation recorder. The power spectrum of the recorded data was observed using a Bruel and Kjaer high resolution signal analyzer, model 2033. Also, a circuit was built to electronically calculate the integral of the individual power spectrum curves over selected frequency ranges. This circuit provides a rapid one number characterization of the Doppler spectrum. A block diagram of the implemented function is shown in Figure 4, and Figure 3 schematically shows the complete experimental set up.

Results

Figure 5 presents the power spectra for three different flow situations in the finger: normal temperature skin, heated skin, and occluded flow. The finger skin is heated by placing the hand in a 44°C water bath for a few minutes, and then the finger is clamped in a lukewarm water bath while measurements are taken. Occluded flow is achieved by inflating a sphygmomanometer above the elbow to a pressure of 200 mm Hg. The spectra show that for heated skin the back-scattered Doppler signal is much greater in amplitude than that for normal temperature skin, and the occluded flow signal is smaller in amplitude.

Figures 6 and 7 show the audio output of the ultrasound instrument and the output of the circuit which calculates the area under the power spectrum respectively when a pressure cuff is alternately inflated and deflated and the finger has been heated. Note the pulsatile component synchronous with the cardiac cycle present in the audio output of the ultrasound instrument; this will be discussed in greater detail below. The input to the integrating circuit is band-

limited to 10 to 100 Hz in order to eliminate some of the effects of the pulsatile component in the data. Both figures show marked change in output that occurs when the cuff is inflated or released.

The above data was taken with the receiver gate set at a depth of 0.7 mm. Figure 8 compares spectra taken at varying depths within the skin. Curve A is typical of depths ranging from 0.24 mm to less than 0.7 mm, curve B is a typical power spectrum of data from depths around 0.7 mm, and curve C is typical of depths greater than 0.7 mm to about 1.7 mm. Note that spectra for data taken from depths in skin less than 0.7 mm have more power at high frequencies (greater than 10 Hz) than those at depths greater than 0.7 mm, and that the 0.7 mm depth has its own unique shape.

Interpretation

Good physical models for ultrasonic measurement of skin blood flow are difficult to obtain, and almost no theoretical calculations have been done to model the scattering from the skin. Some theoretical modeling for laser Doppler scattering has been done by Bonner and Nossal [9], however. They conclude that the laser Doppler power spectrum is either exponential or Gaussian with frequency, depending on the amount of multiple scattering. Since the wavelength of our 20 MHz ultrasound is more than two orders of magnitude larger than that of the He-Ne laser light used in the laser Doppler work, we should not expect Bonner and Nossal's model to apply in our case. In fact, the shape of the ultrasound power spectra which we have measured is exponential when plotted on a log scale ($\log[P(f)] = Ae^{-\alpha f} + C$).

One can make some initial hypotheses and calculations, however, to give insight into the characteristic shape of the ultrasonic Doppler power spectrum. The highest frequency components in the spectrum should be related to the maximum velocities of red blood cells in the vessels of the skin. Table 3 gives the maximum Doppler shift frequencies corresponding to common velocities in the vessels of the skin [10]. The table shows that the Doppler spectrum is limited to the 0 to 100 Hz frequency range, and the mean velocities give Doppler shifts well below 50 Hz.

One can also assume that the blood cells in some of the vessels under observation move with a pulsatile velocity. To model this phenomenon in a simple way we assume that the blood velocity as a function of time is given by:

$$V(t) = v_o + \beta v_o \cos(\omega_p t) \tag{1}$$

where β is the fractional change in the mean velocity, v_o, of blood cells in a single vessel, and $\omega_p = 2\pi f_p$, where f_p is the pulse rate. An ultrasonic wave scattered from an object with this motion gives an output from the ultrasound instrument of the form

$$\begin{aligned} E_d(t) = {} & J_o(m_f)\cos(\omega_o t) + J_1(m_f)[\cos(\omega_o + \omega_p)t - \cos(\omega_o - \omega_p)t] \\ & + J_2(m_f)[\cos(\omega_o + 2\omega_p)t + \cos(\omega_o - 2\omega_p)t] \\ & + J_3(m_f)[\cos(\omega_o + 3\omega_p)t - \cos(\omega_o - 3\omega_p)t] + \cdots \end{aligned} \tag{2}$$

where $J_n(m_f)$ is a Bessel function of the first kind,

$$m_f = \beta \frac{\omega_o}{\omega_p} \text{, and } \omega_o = \frac{2\omega_i v_o \cos\theta}{c} \quad .$$

The expression for ω_o is the Doppler shift equation where ω_i is the incident wave frequency, c is the velocity of propogation, and θ is the angle between the direction of propagation of the incident wave and the velocity of the particle.

Equation 2 has the form of a frequency modulated spectrum, which is a set of symmetrical impulse functions centered about ω_o and separated from one another by ω_p. Equation 2 gives a spectrum for a single scatterer, however, the actual signal is composed of an ensemble of signals scattered from cells in different vessels, each with a different mean velocity v_o and angle θ. Thus, the total back-scattered signal will be a sum of a set of E_d's. The power spectrum of the output will then become one continuous or smeared out curve with no visible harmonic structure due to the pulsatility of the velocity of blood cells.

Moving interfaces within the skin could give an FM signal output centered about $\omega_o = 0$ ($v_o = 0$) if relative motion between the stratum corneum and the interface exists. The motion would be in synchronism with the heart rate and would thus give impulses in the power spectrum at $\omega = 0, \omega_p, 2\omega_p, 3\omega_p, \cdots$. Broadened impulses at these frequencies do appear in Figures 5 and 8, but this interface motion would be characterized by phase variations in the Doppler audio output. Our output signals, however, are dominated by large amplitude variations in synchronism with the heart cycle, as shown in Figure 6.

The amplitude changes may also be caused by the partial filling and emptying of the skin microvasculature with blood during each cardiac cycle, causing an accompanying change in density of scatterers. Clearly, the Fourier transform of a function of this form, which is periodic with the heart rate, will include components at the heart rate ω_p, as well as its harmonics. This plethysmographic (amplitude modulation) component should also be investigated as the source of peaks in the power spectra shown at 1, 2, 3, $\cdots$ Hz.

The final consideration in this analysis of the shape of the Doppler power spectrum is the random orientation of vessels in the skin. First we need to restate the basic Doppler shift equation:

$$\Delta f = \frac{2vf_i \cos\theta}{c} \qquad (3)$$

where Δf is the Doppler shift frequency, f_i is the incident wave frequency, and v is the velocity of a scatterer. One can see that the cos θ term in the equation will have a large effect on the distribution of Doppler shifted frequencies in a randomly oriented system.

In order to clarify the effect of this term, assume that the time averaged number of blood cells in the i'th blood vessel in the acoustic sample volume, having velocity v, can be represented by a gaussian curve (Figure 9a) of the form:

$$N_i(v) = \frac{a_i}{\sigma_i\sqrt{2\pi}} \exp\left[\frac{-(v-\bar{v}_i)^2}{2\sigma_i^2}\right] \quad (4)$$

where a_i is the total, time averaged number of cells in the i'th vessel in the sample volume, and σ_i is the standard deviation from the mean velocity $\bar{v}_i$ in the i'th vessel. The velocity distribution function for a number vessels in the skin is then simply the sum of all the $N_i(v)$'s:

$$N(v) = \Sigma\, N_i(v)$$

and is shown in Figure 9a. If all the vessels in the skin were oriented vertically, the Doppler frequency spectrum would have the same shape as N(v) since Δf is proportional to v (eq. 3). However, since the i'th vessel is oriented at an angle θ_i, which varies randomly between 0 and 90°, the velocity distribution $N_i(v)$ for the i'th vessel must be modified. The i'th distribution is changed by multiplying $\bar{v}_i$ and σ_i by cos θ_i. The modified velocity distribution function $N_i^*(v)$ shown in Figure 9b has the same shape as $N_i(v)$, but is shifted towards smaller velocities. $N_i^*(v)$ is a much narrower curve since σ_i is multiplied by cos θ_i. The σ_i^{-1} factor in $N_i(v)$ also causes the amplitude of $N_i(v)$ to increase by 1/cos θ_i. This maintains constant area under the $N_i(v)$ and $N_i^*(v)$ distributions. Physically, since the number of scatterers moving through each vessel stays the same, the area under each $N_i^*(v)$ curve must be the same as that under the $N_i(v)$ curve. For θ_i's close to 90°, cos θ_i is small. Thus, the closer each $N_i(v)$ is shifted towards zero velocity, the taller and narrower $N_i^*(v)$ will be. The sum of all the $N_i^*(v)$ gives the actual velocity distribution function that the Doppler ultrasound instrument observes:

$$N_{obs}(v) = \Sigma\, N_i^*(v)$$

Figure 9b shows the observed velocity distribution function. The Doppler shifted frequency spectrum will then be the same shape as that of $N_{obs}(v)$: a function of large amplitude around OHz, decaying as frequency increases.

Support for the angle effect on velocity distribution can be obtained by aiming the transducer at a 24 ga. teflon tube containing a flowing solution of water and scatterers (GE Anti-foam emulsion). Figure 10 shows how the shape of the power spectrum varies with respect to the angle between the flowing solution and the transducer. As the angle approaches 90° the spectrum shifts toward lower frequencies as predicted.

The above discussion demonstrates that vessels lying transversely in the skin (angle between transducer and vessel approaching 90°) will add significantly to the power spectrum at very low frequencies. The shape of the power spectral density curves measured at each depth in the skin is governed by the angular distribution of the vessels and their size distribution. Specific microvascular structures such as capillary beds and arteriolar and venous plexi are expected to have characteristic Doppler spectrum signatures.

Conclusion

Experimental results show that changes in the output of a pulsed Doppler ultrasound flow detector can be produced by normal reactions of skin to physiological stimuli. The changes in the output are evident in the power spectrum, and in an electronically produced integral of the spectrum. Power spectrum

curve shape has also been shown to be a possible indicator of the vascular structures within the skin. A plethysmographic component has been shown to exist in the output that correlates with the pulsatility of the blood flow. Work is continuing in defining the type of scattering that occurs in the skin, and in establishing characteristic Doppler signatures for different microvascular skin structures found at different depths.

[1] David M. Heimbach, Martin A. Afromowitz, Mark Hoeffner, Mark Burns, and Loren H. Engrav, "Burn Depth Indicator," Am. Burn Assoc. 12th Ann. Mtg., San Antonio, March, 1980.

[2] John E. Chimoskey and William Flanagan, "Ultraviolet-induced cutaneous hyperemia measured by Xenon 133 in man," J. Invest. Derm, vol. 63, no. 4, pp. 367-368

[3] A. C. Burton, "The range and variability of the blood flow in the human fingers and the vasomotor regulation of body temperature," American J. Physiology 127: 437-453, 1939

[4] Gert E. Nilsson and Torsten Tenland, "Evaluation of a laser Doppler flowmeter for measurement of tissue blood flow," IEEE Transactions on Biomedical Engr., BME-27 (1980), 597

[5] Gert E. Nilsson and Torsten Tenland, "A new instrument for continuous measurement of tissue blood flow by light beating spectroscopy," IEEE Trans. on Biomed. Engr., BME-27 (1980), 12

[6] Dennis Watkins and G. Allen Holloway, "An instrument to measure cutaneous blood flow using the Doppler shift of laser light," IEEE Trans. on Biomed. Engr., BME-25 (1978), 28

[7] R. W. Wunderlich and R. L. Folger, "Laser Doppler blood flow meter and optical plethysmograph, " Rev. Sci. Instr., 51 (1980), 1258

[8] 20 MHz pulsed Doppler, PD-117. Built by Craig J. Hartley, Baylor College of Medicine, Houston, Texas

[9] R. Bonner and R. Nossal, "Model for laser Doppler measurements of blood flow in tissue," Applied Optics, Vol. 20, No. 12, pp 2097-2107

[10] Arthur Jarret. The Physiology and Pathology of the Skin. New York: Academic Press, 1973

Table 3

Blood Cell Velocity and Corresponding Doppler Shift for 20 MHz Ultrasound

Vessel Type	Expected Range		Mean	
	Velocity mm/s	Doppler Shift (Hz)	Velocity mm/s	Doppler Shift (Hz)
Arteriole	0.68 - 3.87	17 - 98	1.50	38
Capillary	0.23 - 1.48	6 - 38	0.74	19
Venules	0.32 - 1.21	8 - 31	0.66	17
Arteriole-Venular Shunt	0.38 - 2.22	10 - 56	1.37	35

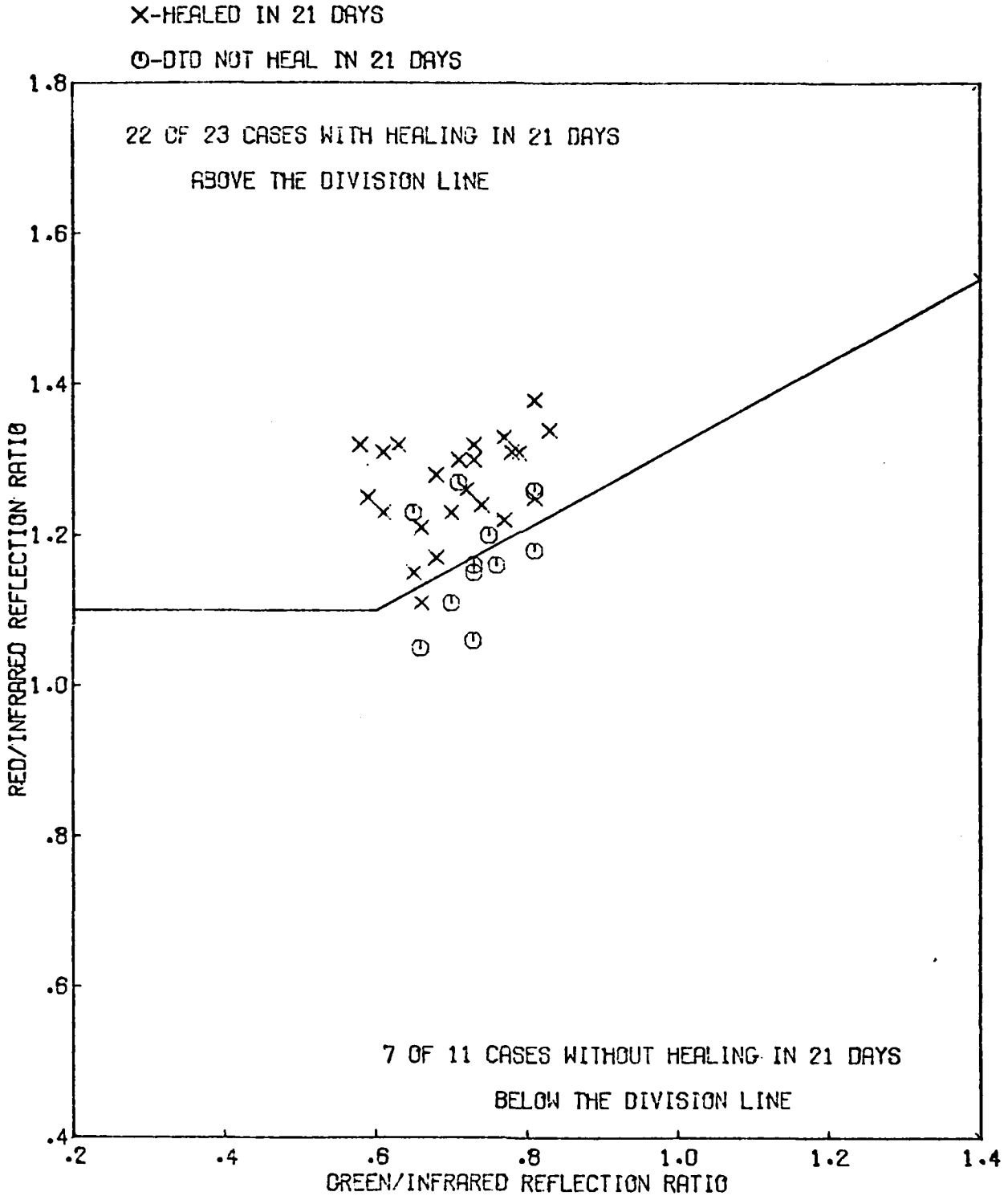

HANDS/FEET, DAY 2, CLIN. EVALUATION: WILL HEAL

Figure 1

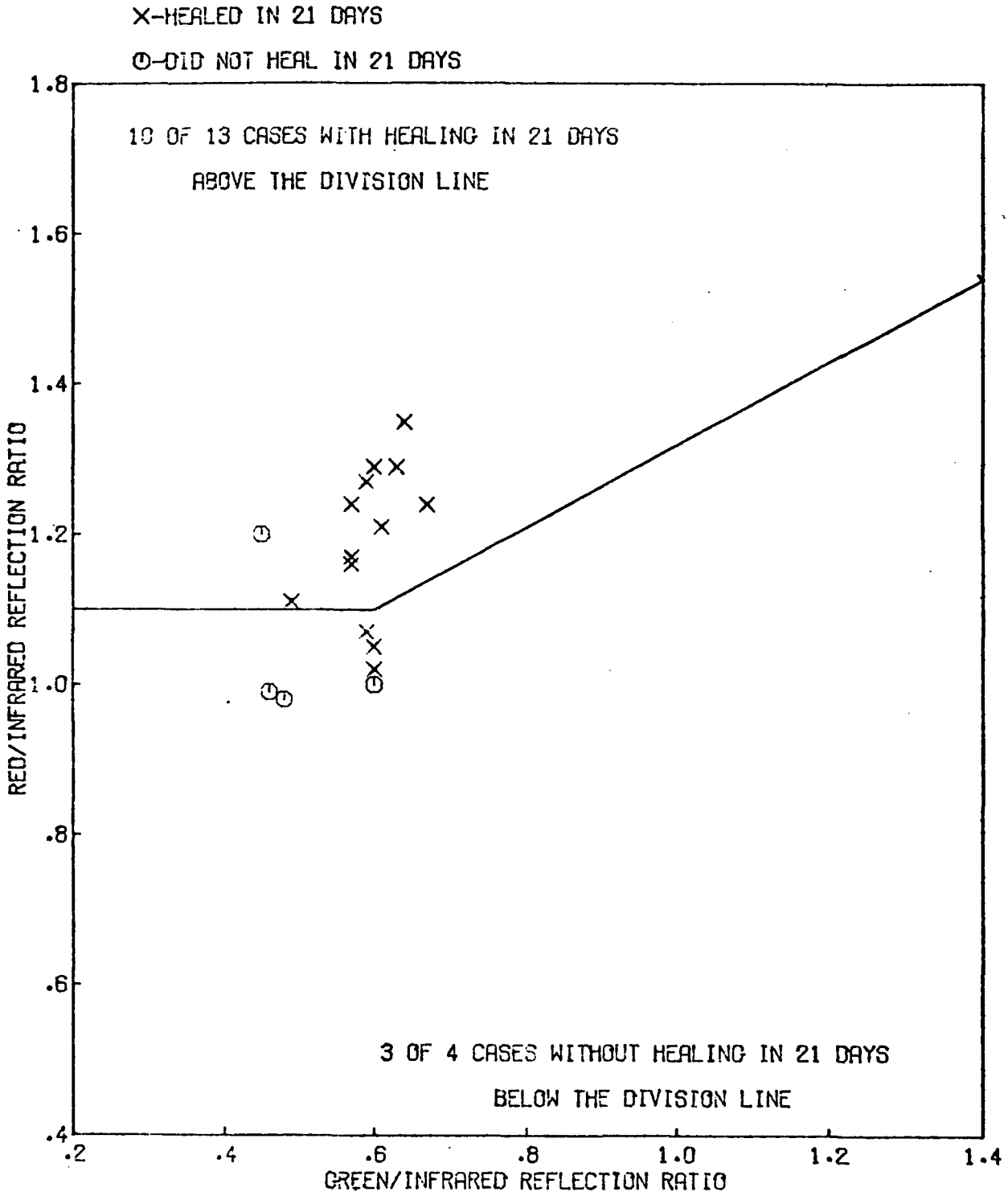

HANDS/FEET, DAY 2, CLIN. EVALUATION: DON'T KNOW

Figure 2

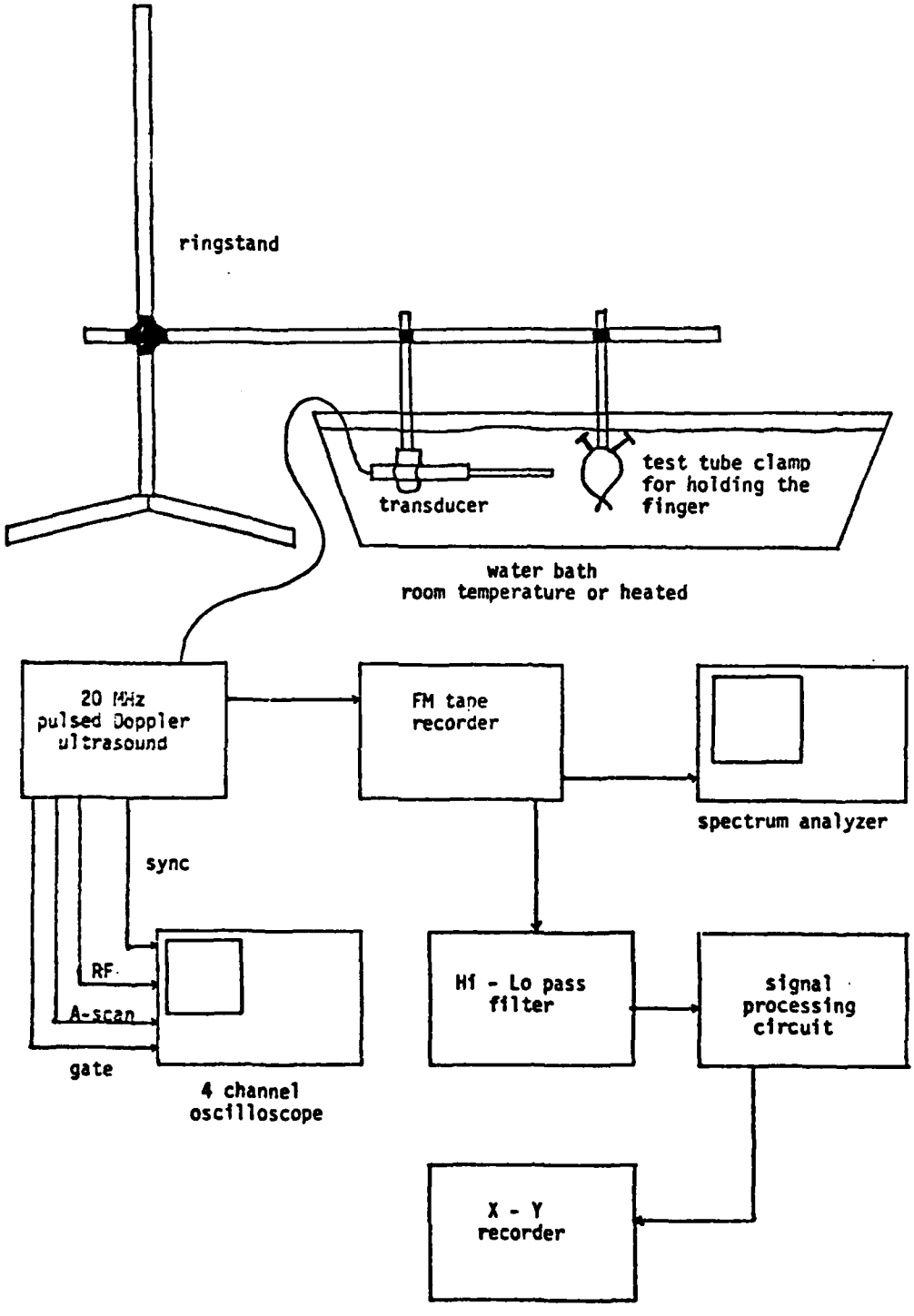

Figure 3: Experimental setup.

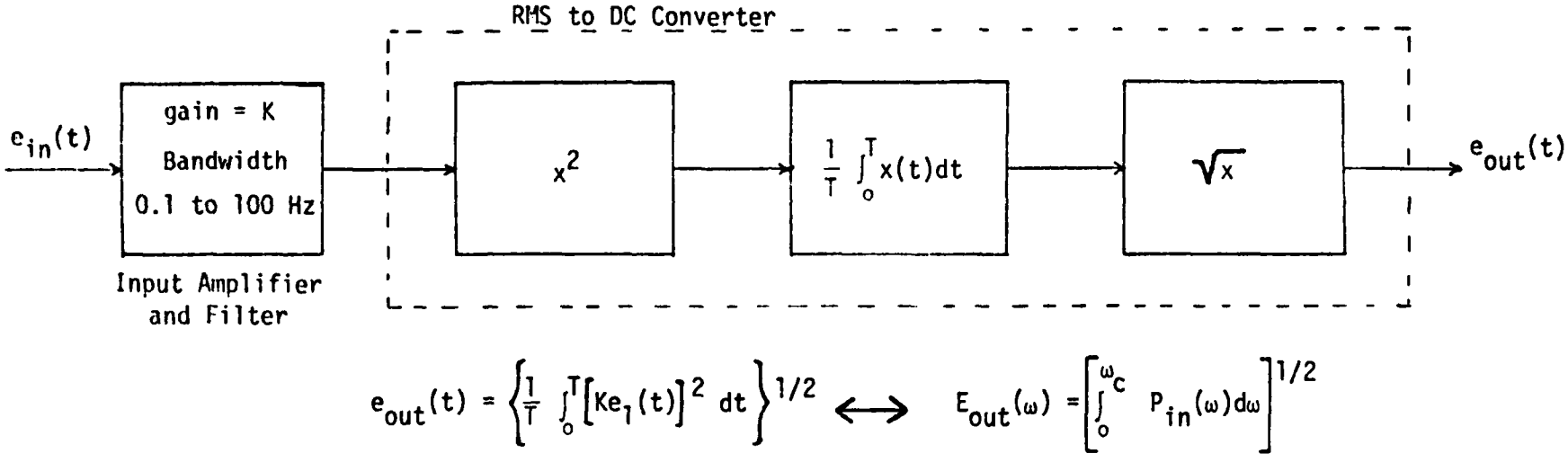

Figure 4: Block diagram of the electronic integral of the power spectrum.

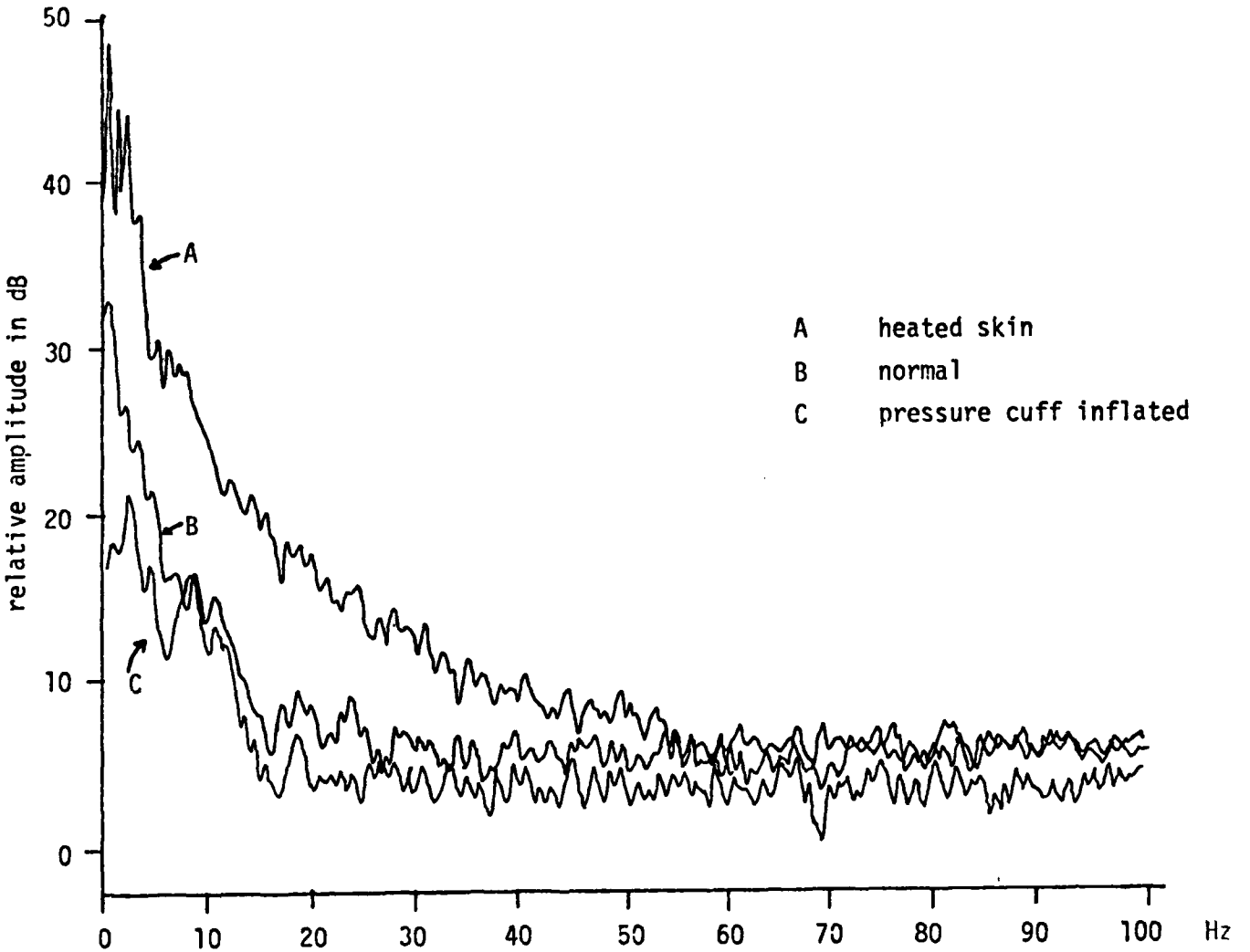

Figure 5: Power spectra of data taken from heated skin, normal skin, and when a pressure cuff is used.

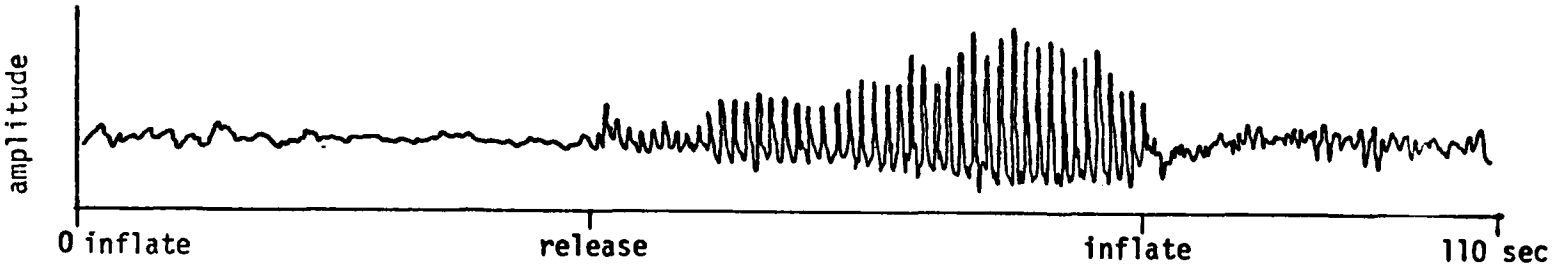

Figure 6: Audio output signal from the ultrasound instrument when a pressure cuff is alternately inflated and released. Note the peaks that occur in the output synchronous with the heart cycle.

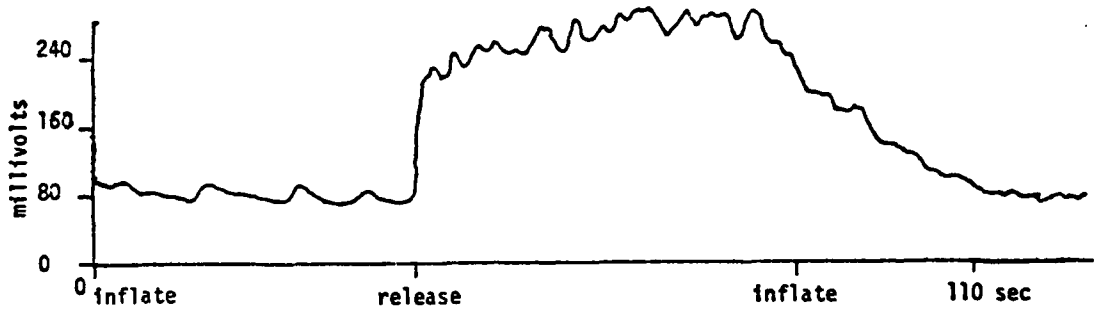

Figure 7: Electronic integral of the Doppler power spectrum versus time when a pressure cuff is alternately released and inflated. Bandwidth 10 to 100 Hz.

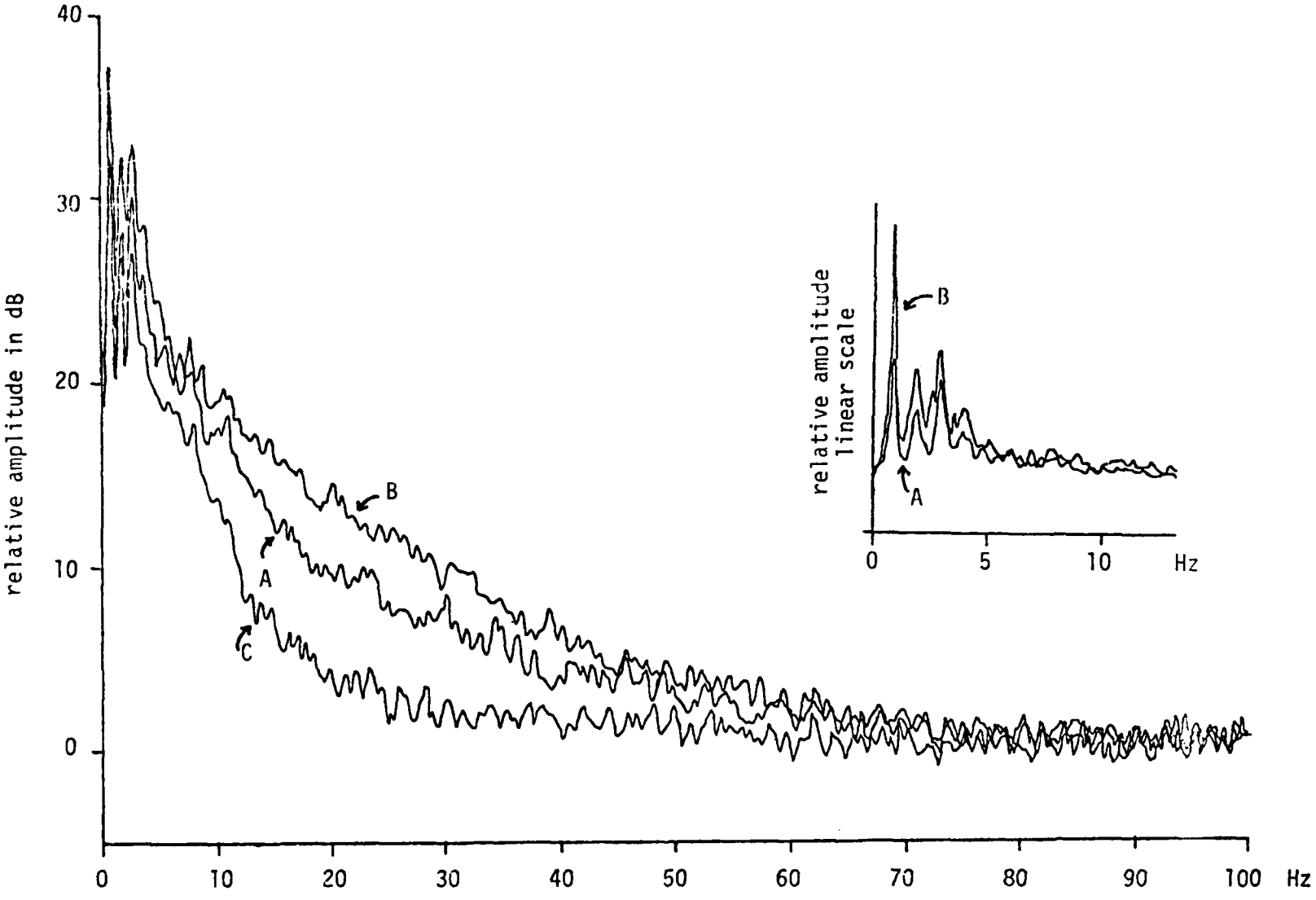

Figure 8: Power spectra from three depths in the skin: A, 0.7mm; B, 0.24 to 0.7mm; C, 0.7 to 1.7mm. Inset shows curves A and B for low frequencies on a linear scale; peaks are at 1, 2, 3, and 4 Hz, harmonics of the heart rate.

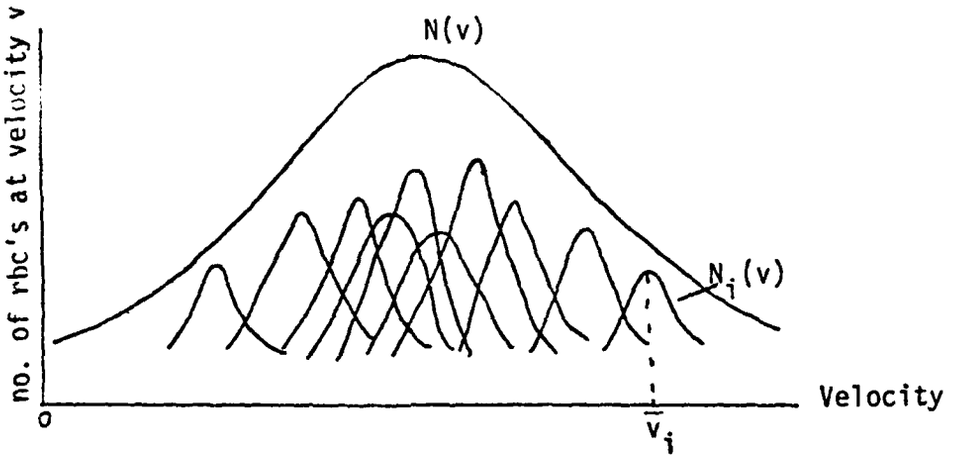

a. Velocity distribution of blood cells in an ensemble of vessels.

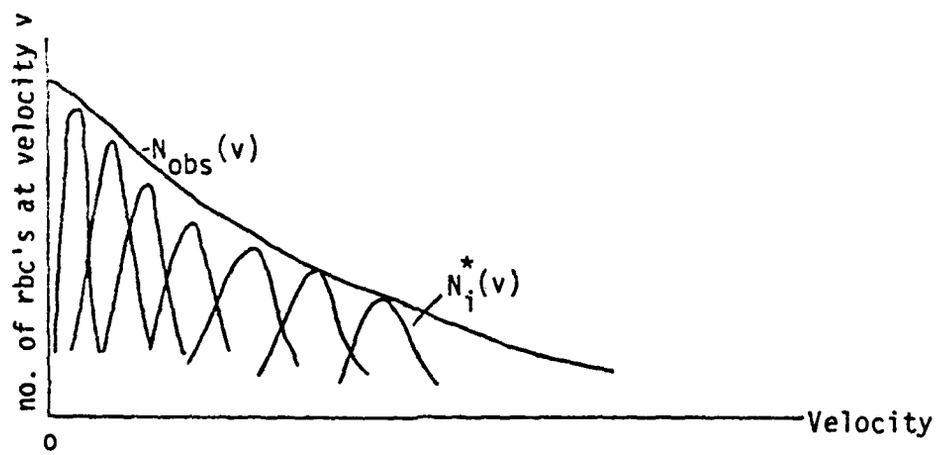

b. Observed velocity distribution of blood cells due to the random orientation of vessels in the skin. Power spectrum has the same shape as $N_{obs}(v)$.

Figure 9 : Doppler power spectrum shape.

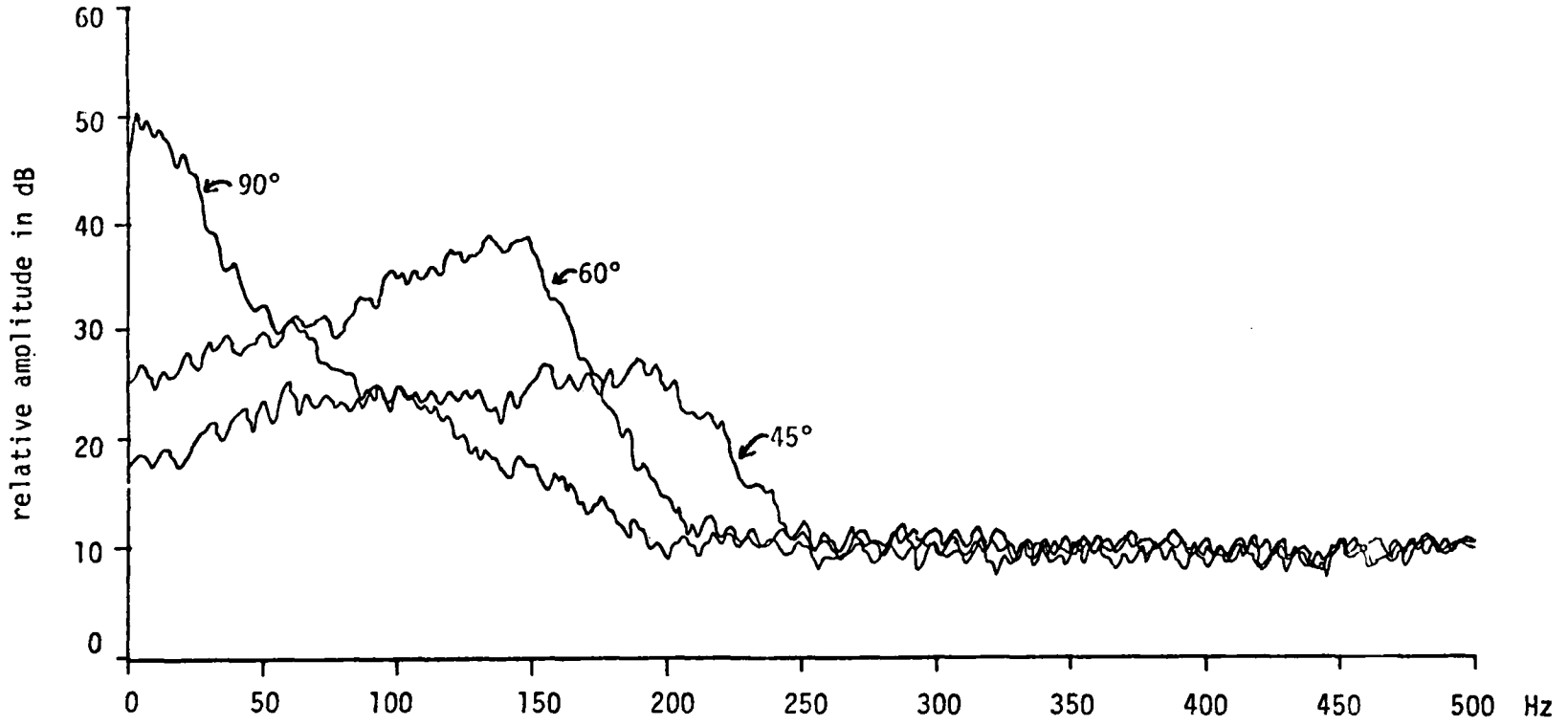

Figure 10: Power spectra of the Doppler signal from a flowing solution of scatterers in a tube for three angles between the transducer and tubing.

END

DTIC

6-86